Stable, Low-Temperature Discotic Nematic Superstructures by Incorporating a Laterally Substituted Sidearm in Hexakis(phenylethynyl)benzene Discogens

ARTICLE *in* ADVANCED FUNCTIONAL MATERIALS · AUGUST 2007

Impact Factor: 11.81 · DOI: 10.1002/adfm.200601019

7 AUTHORS, INCLUDING:

Hsiu-Fu Hsu
Tamkang University
57 PUBLICATIONS **1,053** CITATIONS

SEE PROFILE

ADVANCED FUNCTIONAL MATERIALS

FULL PAPER

DOI: 10.1002/adfm.200601019

Stable, Low-Temperature Discotic Nematic Superstructures by Incorporating a Laterally Substituted Sidearm in Hexakis(phenylethynyl)benzene Discogens**

By *Shih-Chien Chien*, *Hsiu-Hui Chen*, *Hsin-Chou Chen*, *Yu-Ling Yang*, *Hsiu-Fu Hsu*,* *Tzenge-Lien Shih*, and *Jey-Jau Lee*

A new strategy for preparing room-temperature discotic nematic materials is proposed and developed stepwise to improve various discotic nematic properties. This approach replaces one sidearm of the discotic hexakis(4-hexyloxyphenylethynyl)benzene with a tris(alkoxy) sidearm, 1-ethynyl-2,3,4-tris(hexyloxybenzene), to lower transition temperatures, manipulate discotic nematic ranges, and preserve the discotic nematic superstructure while preventing column formation. Although symmetry considerations play a role in the resulting mesogenic properties, steric hindrance and van der Waals interactions are ascribed to the superior discotic nematic properties of the newly prepared discogens containing a laterally substituted sidearm.

1. Introduction

Disclike molecules exhibiting a nematic mesophase have drawn much attention recently as materials in compensating films[1] or as potential materials in a liquid-crystalline layer to improve the viewing-angle characteristics of liquid-crystalline displays.[2] Compared to the mass number of calamitic nematogens, there have only been a few disclike molecules reported that exhibit the discotic nematic (N_D) phase.[2,3] Among the discotic nematogens, multiynylbenzenes[3c–f] have been the most investigated system. Often, disclike molecules are prone to forming columnar (Col) mesophases because of the strong interdisc interactions, such as π–π interactions, from the planar core structures. For multiynyl compounds, however, the rotational freedom provided by the ethynyl linkers thwarts efficient stacking of the discs and hence reduces interdisc interactions, preventing column formation. Unfortunately, N_D phases are typically accompanied by narrow mesophase ranges and high transition temperatures, especially high melting points.[3] To realize practical applications, room-temperature N_D materials with reasonable ranges are required. Recently, a room-temperature N_D phase[2] was achieved for hexakis(4-alkylphenylethynyl)benzene by introducing racemic branched alkyl side chains that provided stereoheterogeneity, which generated a mixture of different components. Thus, a low melting point (T_m) was obtained by preparing a eutectic mixture; however, a single component N_D material with an ambient melting temperature is yet to be achieved.

To obtain desired molecular superstructures, specifically the discotic nematic packing motif, a delicate balance of complex intermolecular interactions is necessary. By examining the packing motif of the crystal structure of hexakis(4-hexyloxyphenyl)ethynylbenzene (**1**)[4] reported by Grubbs, intermolecular interactions of the disclike molecules in the solid-state can be realized. The discs are approximately parallel to each other. For each disc, one peripheral phenyl ring is found to have short contacts of 3.5 Å and offset face-to-face π–π interactions with two peripheral phenyl rings, one from the disc above and one from the disc below. By moving from the solid-state into a liquid-crystalline state, the weak intermolecular interactions on the periphery are expected to be further weakened by the aforementioned rotational freedom to form an N_D phase instead of a columnar phase. Hence, increasing the intermolecular interactions on the periphery rather than for the whole disc should lead to a wider range of N_D superstructures while avoiding column formation.

Lateral substitutions have been utilized in calamitic mesogens to favor the formation of the nematic phase, to depress lamellar structures, and more importantly, to significantly lower the transition temperatures.[5] Similarly, V-shaped mesogens with laterally substituted chains were also found to favor the formation of nematic phases.[6] However, only a few examples have been reported for discotic systems with lateral substitutions.[7] In the case of triphenylen-2,3,6,7,10,11-hexayl hexakis(4-alkoxybenzoate), lateral substitution in the peripheral phenyl rings was utilized to enhance the discotic nematic stability by suppressing the columnar mesophases.[7c] The opposite trend for the clearing temperatures, namely decreasing temper-

[*] Prof. H.-F. Hsu, S.-C. Chien, H.-H. Chen, H.-C. Chen, Y.-L. Yang, Prof. T.-L. Shih
Department of Chemistry
Tamkang University
Tamsui 25151 (Taiwan)
E-mail: hhsu@mail.tku.edu.tw
Dr. J.-J. Lee
National Synchrotron Radiation Research Center
Hsin-Chu 30076 (Taiwan)

[**] This work was supported by a grant from the National Science Council of Taiwan (NSC 94-2113-M-032-009).

ADVANCED FUNCTIONAL MATERIALS

ature with increasing size of the lateral substitution, was found for compounds with the lateral groups *meta* and *ortho* to the ether linkage. In contrast, no obvious effects could be seen for the melting points for either substitution patterns. In this context, an effective way to achieve both low temperature and stable N_D materials is to laterally substitute one sidearm onto a hexaynylbenzene core. The aforementioned restricted rotation of the laterally substituted sidearm should enhance π–π interactions on the periphery of the disc to stabilize the existing N_D phase. Contrastingly, the protrusion of the introduced lateral substitution off the disc plane should prevent column formation by discouraging face-to-face packing motifs. Furthermore, lateral substitution in the peripheral phenyl rings *ortho* to the ethynyl group should lead to significantly lowered transition temperatures.

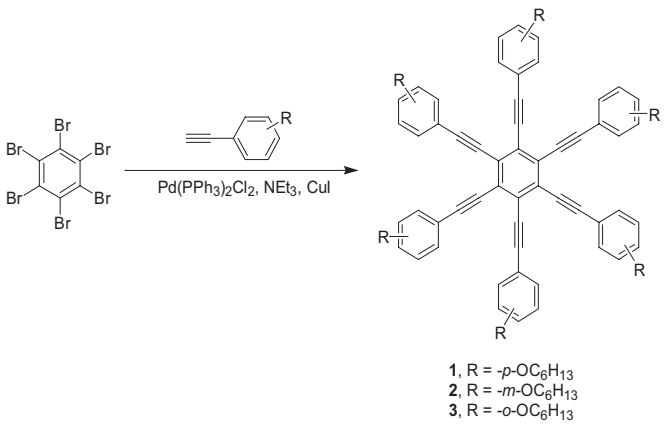

Scheme 1. Synthesis of compounds **1**, **2**, and **3**.

2. Results and Discussion

To verify this theory, the alkoxy chains of **1** were shifted from the *para*- to the *meta*- or *ortho*-positions with respect to the ethynyl group. Three types of sidearms, 1-ethynyl-4-hexyloxybenzene (*para*-sidearm), 1-ethynyl-3-hexyloxybenzene (*meta*-sidearm), and 1-ethynyl-2-hexyloxybenzene (*ortho*-sidearm), were coupled to hexabromobenzene to afford **1**, **2**, and **3**, respectively, as shown in Scheme 1. Although **1** was previously reported by Grubbs, its mesogenic properties were not described. This *para*-derivative exhibited an N_D phase between 144 and 216 °C. In contrast, neither **2** (mp 87 °C) nor **3** (mp 63 °C) demonstrated mesogenic properties. Nevertheless, significantly lowered melting points were achieved by shifting the positions of the alkoxy chains of the six sidearms. Moreover, the decrease in T_m along the *para*-, *meta*-, *ortho*-derivative series is encouraging and will be important for the following investigations.

A decrease in the number of laterally substituted sidearms was attained in order to regain the N_D phase. Grafting two *ortho*-sidearms onto 1,3-dibromo-2,4,5,6-tetrakis(4-hexyloxyphenylethynyl)benzene afforded **4** (Scheme 2), which was still not liquid crystalline with a m.p. of 85 °C. Further reducing the number of *ortho*-sidearms to one by coupling one *ortho*-sidearm with 1-bromo-2,3,4,5,6-pentakis(4-hexyloxyphenylethynyl)benzene yielded **5**, which exhibited an N_D phase between 87 and 100 °C, as shown in Table 1. By comparing the thermal behaviors of **1**, **5**, **4**, and **3**, which have zero, one,

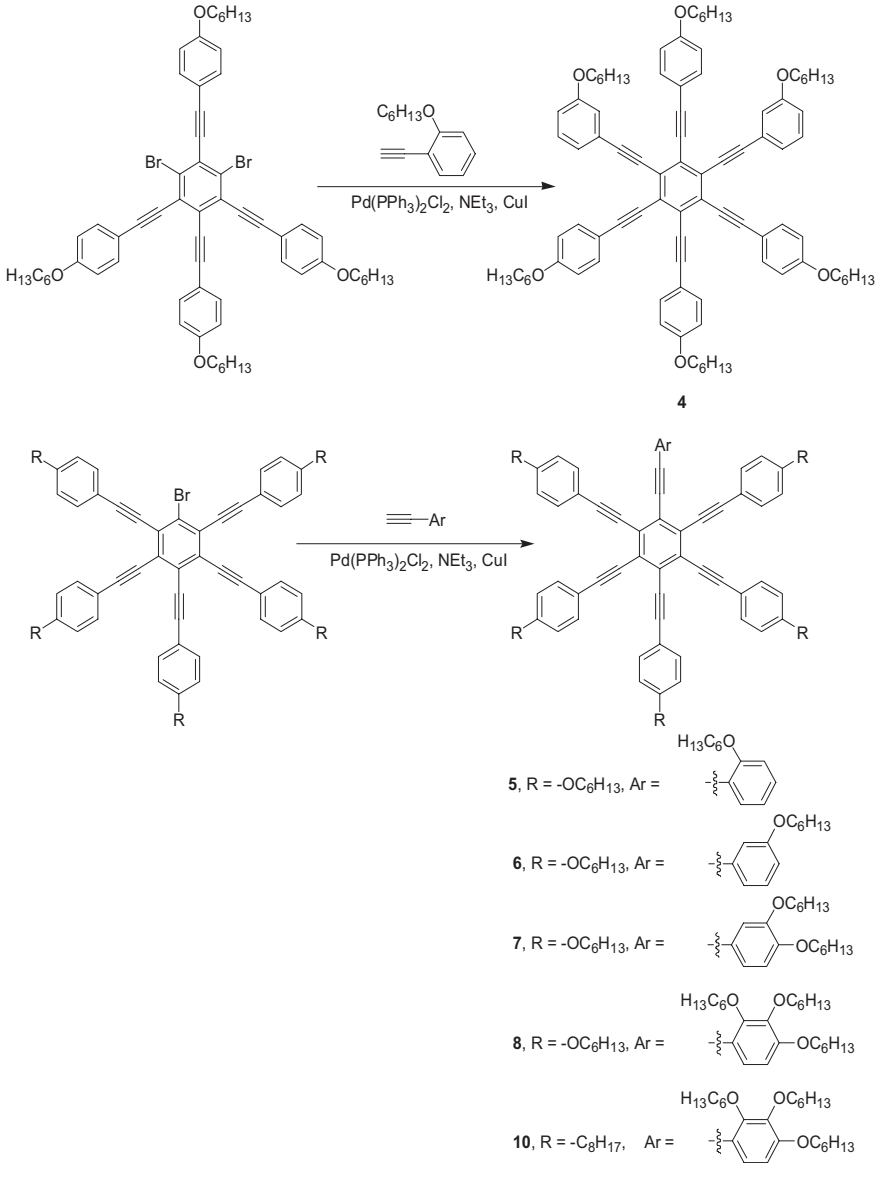

Scheme 2. Synthesis of compounds **4**, **5**, **6**, **7**, **8**, and **10**.

Table 1. Phase behaviors of compounds **1**, **5**, **6**, **7**, **8**, and **10**.

Compound	Phase behaviors [a]
1	K $\xrightarrow{143.5\ (37.73)}$ N_D $\xrightarrow{215.9\ (0.05)}$ $I_{partial\ decomp.}$
5	K $\underset{46.8\ (-41.18)}{\overset{87.3\ (51.00)}{\rightleftharpoons}}$ N_D $\underset{99.3\ (-0.16)}{\overset{100.0\ (0.19)}{\rightleftharpoons}}$ I
6	K $\xrightarrow{108.8\ (62.14)}$ N_D $\xrightarrow{178.5[b]}$ $I_{partial\ decomp.}$
7	K $\xrightarrow{93.7\ (65.72)}$ N_D $\xrightarrow{195.0[b]}$ $I_{partial\ decomp.}$
8	K $\underset{60.5\ (-41.83)}{\overset{83.0\ (41.95)}{\rightleftharpoons}}$ N_D $\underset{118.6[b]}{\overset{120.6[b]}{\rightleftharpoons}}$ I
10	K $\underset{22.0\ (-37.60)}{\overset{30.2\ (38.46)}{\rightleftharpoons}}$ N_D $\underset{59.7\ (-0.17)}{\overset{60.8\ (0.22)}{\rightleftharpoons}}$ I

[a] The transition temperatures (°C) and enthalpies (listed in parentheses, kJ mol^{-1}) were determined by differential scanning calorimetry (DSC) at 10 °C min^{-1}. K is the crystalline phase; N_D is a discotic nematic mesophase; I is an isotropic liquid; $I_{partial\ decomp.}$ is an isotropic liquid with partial decomposition. [b] From polarizing optical microscopy (POM).

two, and six *ortho*-sidearms, respectively, it was found that the melting point drastically decreased with the substitution of only one *ortho*-sidearm, and this trend, in which the melting temperature is lowered, was slowed with the substitution of additional *ortho*-sidearms. We found that the descending transition-temperature effect must be more pronounced for clearing temperatures than for melting points to result in the severe shrinkage of the N_D range for **5** and the disappearance of the N_D phases in **3** and **4**.

In order to improve the decreased N_D range of **5**, one of the sidearms in **1** was replaced with a sidearm in the *meta* position to give **6**, which exhibited an N_D phase between 109 and 179 °C. The modification that resulted in **6** caused both the melting and clearing points to be lowered to a similar extent, 35 and 37 °C, respectively, yielding a mesophase range similar to **1**. Comparing the mesogenic properties of **1**, **6**, and **5**, we found that incorporating a *meta*-sidearm gave a moderate decrease in the melting and clearing points while preserving the mesophase range. In contrast, with one *ortho*-sidearm, although the melting point decreased to a large extent, the clearing point was lowered even more to give a narrow mesophase range. Symmetry considerations could be accountable for the lower transition points for **5** and **6**; however, the different extents to which the temperatures decreased for **5** and **6** suggest that symmetry is not the sole factor. In addition to the symmetry consideration, the steric hindrance of the laterally attached alkoxy chain seemed to contribute significantly to the lower transition temperatures.

Compound **1**, with all *para*-sidearms, exhibited the highest clearing temperature and the widest mesophase range among compounds **1**–**6**; in contrast, replacing one sidearm in **1** with a *meta*-sidearm afforded **6**, which demonstrated a much lower melting point and a preserved mesophase range. In order to further maneuver the mesogenic properties, **7**, with the unique sidearm 4-ethynyl-1,2-bis(hexyloxybenzene), was prepared in the hopes of retaining the favorable properties of **1** and **6**—that is, the low melting point of **6** and the high clearing temperature of **1** (i.e., a wider mesophase range). It was expected that the rotation of the unique sidearm would be further restricted to increase intermolecular sidearm–sidearm interactions to promote liquid crystallinity. Moreover, with one more alkoxy chain, the increased van der Waals interactions among chains should also favor intermolecular interactions; meanwhile, the *meta*-attachment of the additional chain should provide steric hindrance to prevent the formation of columnar superstructures. Hence, the additional lateral substitution in **7** should give rise to less nanosegregation of the chains, hence impeding columnar phase formation. The mesogenic properties of **7** are also shown in Table 1. Interestingly, the melting point of **7** was lower than for **1** and **6**. More importantly, the mesophase range of **7** was much wider than the ranges exhibited by **1** and **6**. These results prompted us to incorporate the unique sidearm, 1-ethynyl-2,3,4-trishexyloxybenzene, which has three adjacent *para*-, *meta*- and *ortho*-alkoxy chains, onto **8**, as shown in Figure 1. The melting point was further lowered to 83 °C, whereas the clearing temperature was also lowered but to a more significant extent, to 121 °C, hence yielding a smaller but acceptable N_D range of 38 °C. Apparently, the small mesophase range caused by attaching an *ortho*-chain, as observed in the mesogenic behaviors of **5**, also played a significant role in the resulting narrowed N_D range of **8**.

In order to pursue room-temperature N_D materials, the unique sidearm 1-ethynyl-2,3,4-trishexyloxybenzene was employed to replace one sidearm in hexakis(4-octylphenylethynyl)benzene (**9**)[8] to furnish **10**. Compound **9** was targeted from the various previously reported single-component hexaynylbenzenes, as it showed the lowest transition temperatures

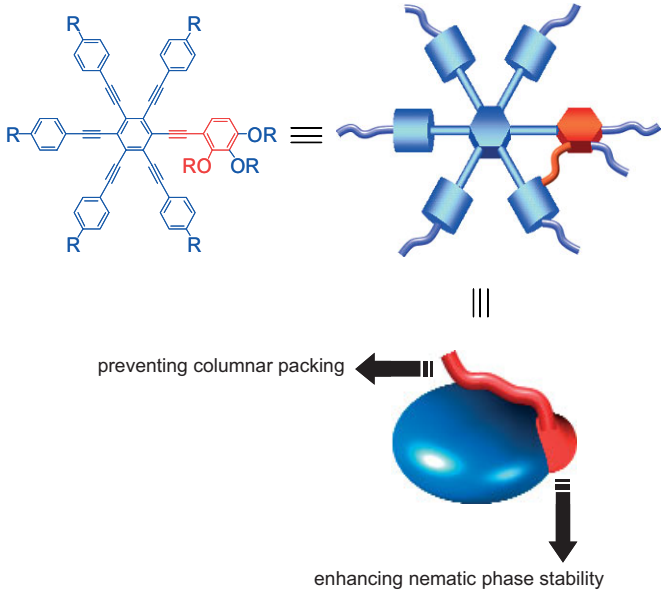

Figure 1. Structure of **8** with a laterally substituted sidearm to prevent columnar packing and enhance discotic nematic phase stability.

ADVANCED FUNCTIONAL MATERIALS

and an N_D phase between 80 and 96 °C. Excitingly, the N_D phase of **10** was determined to be between 30 and 61 °C. Compared to **9**, **10** exhibited an almost doubled mesophase range, and its melting point was 50 °C lower, nearly room temperature. The widened mesophase range could be attributed to the three ether linkages, as it is known that alkoxy derivatives typically show broader ranges than those of alkyl derivatives.[9]

The schlieren textures of **2**–**10** observed from polarized optical microscopy (POM) were indicative of a nematic mesophase, which can be a discotic nematic or a columnar nematic phase. The fact that the thermal fluctuations of these textures were similar to observed fluctuations for the discotic nematic phase of **1** suggests the mesophases of **2**–**10** are discotic nematic.

The identity of the nematic phase of these compounds was determined by powder X-ray diffraction (XRD). XRD patterns of the mesophases of **1** and **8** are shown in Figure 2. The XRD pattern of the discotic nematic phase of **1** shows one distinct reflection in the small-angle regime, one very broad halo in the mid-angle range, and one halo in the wide-angle area. The halo in the mid-angle range was confirmed by a fit to a Lorentzian profile. The calculated *d*-spacing of 21.2 Å for the reflection in the small-angle region approximated the diameter of the discotic unit, 19.30 Å.[10] The spacing of the wide-angle halo was calculated to be 4.6 Å, which was attributed to the liquidlike correlation of the molten chains. The reflection in the mid-angle range corresponded to a distance of 10.0 Å. A similar signal was also reported for an analog[11] with heptyl chains; however, its origin was not clear. For **8**, two distinct reflections in the small- and wide-angle ranges were recognizable. The mid-angle reflection of **1** was not identifiable for **8** with Lorentzian fitting profiles. The small-angle reflection of **8** at 21.3 Å was similar to **1**. The maximum of the halo in the wide-angle range of **8** was apparently shifted to the large-angle direction with respect to **1**. However, the single maximum Lorentzian fitting of this signal revealed its unsymmetrical shape with a shoulder at its wide-angle side. It was analyzed to show splitting into two distinct maxima with a better Lorentzian fit ($R^2 = 0.9951$). Calculated *d*-spacings of the two best-fit peaks were 4.7 and 4.1 Å, which corresponded to the chain correlation and the interdisc correlation for somewhat aggregated discs, respectively. The fact that the reflection corresponding to a spacing of 4.1 Å was detected for **8** but was unattainable for **1** indicates that the structural modification of attaching two lateral chains onto a peripheral phenyl ring most likely induced a moderate aggregation of the hexaynylbenzene discs.

The extent of order within the mesophase, the correlation length l, was calculated from Scherrer's equation $l = 0.89\lambda/(w_{1/2}\cos\theta)$.[12] Here, λ is the wavelength of the incident X-ray beam, $w_{1/2}$ is the full-width at half maximum of the reflection, and θ is the maximum of the reflection. Both $w_{1/2}$ and θ can be obtained by using a Lorentzian fit of the diffraction pattern. For **1**, the calculated correlation lengths for the reflections corresponding to spacings of 21.2 and 4.6 Å were 17 and 8 Å, respectively. For **8**, the correlation lengths for reflections exhibit-

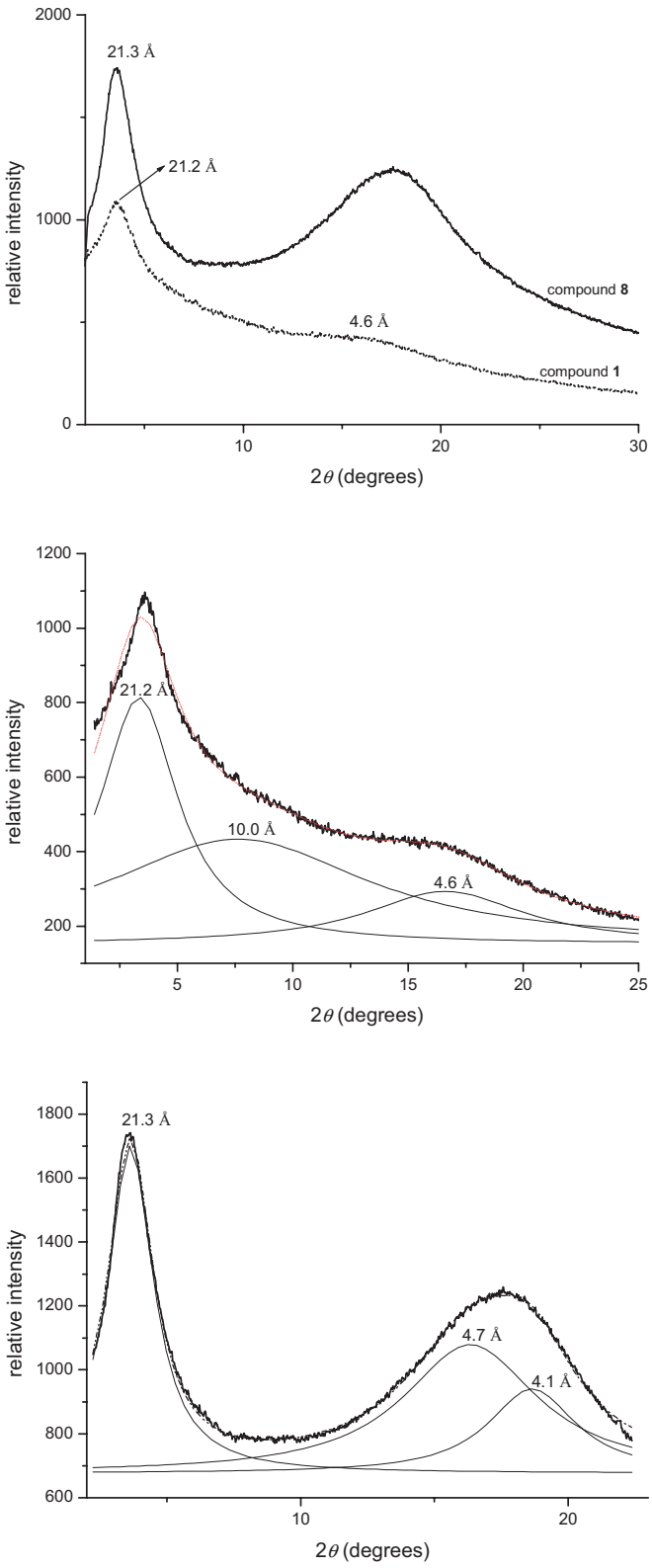

Figure 2. Top: Powder XRD patterns of **1** at 200 °C upon heating and **8** at 100 °C upon cooling. Middle: Lorentzian fits of the XRD pattern of **1** at 200 °C upon cooling. Bottom: Lorentzian fits of the XRD pattern of **8** at 100 °C upon cooling.

ing *d*-spacings of 21.3, 4.7, and 4.1 Å were 33, 11, and 17 Å, respectively. For both compounds, the correlation lengths of the small- and wide-angle regimes were comparable to those lengths reported for the discotic nematic mesophase[13] and were significantly smaller than values for the columnar nematic mesophase.[12c,14] However, it was clear that the correlation lengths for reflections with spacings of 21.3 and 4.7 Å for **8** were significantly larger than the corresponding signals for **1**. The almost doubled correlation length of the small-angle signal for **8** indicates a higher extent of order along the direction perpendicular to the disc normal. For the halo at a spacing of ca. 4.6 Å, although the added chains were laterally attached in **8**, the side-chain correlation of **8** was higher than for **1**. Although absent for **1**, the signal at a spacing of 4.1 Å for **8** may appear from the interaction along the direction parallel to the disc normal within the aggregated ensembles. The correlation length of 17 Å was approximately four disc thicknesses if the discs were stacked to avoid the lateral side chains and roughly three disc thicknesses if the estimated disc thickness included the lateral side chains. Herein, aggregation of discs may imply interactions along the direction parallel to the disc normal. Relative to **1**, structural modification by attaching two lateral chains onto one peripheral phenyl ring as in **8** induced not only a higher correlation of the chains but also a higher extent of order parallel and perpendicular to the disc normal.

Taking into account the POM and XRD results, a discotic nematic phase was unequivocally assigned to the mesophase of **2**–**10**. This assignment was further supported by the considerably small mesophase-to-isotropic transition enthalpies that were similar to those values for discotic nematic phases[13,15] and significantly smaller than values for columnar nematic phases.[12c,16]

Triphenylene compounds have the advantage of showing absorption at wavelengths shorter than 400 nm, rendering them transparent in the visible region, which is important for applications as compensating films.[17] Although the present hexaynylbenzene derivatives **1**–**10** are pale yellow and are not transparent in the visible region, studies of their photophysical properties will provide information about the influence of these structural modifications on the photophysical properties. Photophysical properties of discogens **1**–**10** were studied by UV-visible absorption and fluorescence spectroscopies. Figure 3 shows absorption and emission spectra of **1**, **7**, and **8**. In solution, all three compounds showed similar absorption spectra with a λ_{max} of ca. 365 nm and similar fluorescence spectra with a λ_{max} of 466 nm and a quantum efficiency of ca. 45 %.

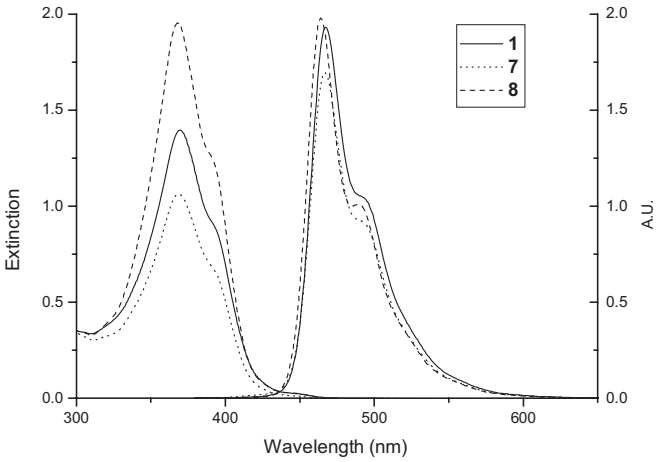

Figure 3. Absorption and fluorescence spectra of **1**, **7**, and **8** in dichloromethane.

3. Conclusions

A new strategy focusing on replacing one sidearm of the discotic hexakis(4-hexyloxyphenylethynyl)benzene with a trisalkoxy sidearm, 1-ethynyl-2,3,4-tris(hexyloxybenzene), has been proposed and developed stepwise to achieve effective improvements in the discotic nematic properties (i.e., lowered transition temperatures and manipulations of N_D ranges while preserving the formation of a discotic nematic superstructure and preventing column formation). The ability to translate these new ideas to other N_D systems is under investigation.

4. Experimental

All chemicals and solvents were reagent grade (Aldrich Chemical Co.) and used without further purification. Compound **1** [6], 1,3-dibromo-2,4,5,6-tetrakis(4-hexyloxyphenylethynyl)benzene [18] and 1-bromo-2,3,4,5,6-pentakis(4-hexyloxyphenylethynyl)benzene [18] were prepared according to literature procedures. ^{1}H and ^{13}C NMR spectra were recorded on a Bruker AC-300 spectrometer. Chemical shifts were reported in parts per million (ppm) relative to residual $CHCl_3$ ($\delta = 7.26$, ^{1}H; 77.0, ^{13}C). Multiplicities were given as s (singlet), d (doublet), dd (doublet of doublets), t (triplet), q (quartet), and m (multiplet). Absorption spectra were recorded with a Jasco V-550 spectrometer. Photoluminescence spectra were recorded with a Hitachi F-2500 fluorescence spectrophotometer. Differential scanning calorimetry (DSC) data were obtained on a Perkin-Elmer Pyris1 with heating and cooling rates of 5 and 10 °C min^{-1}. POM was carried out on a Nikon Eclipse E600 POL with a Mettler FP90/FP82HT hot-stage system. Powder XRD data were collected on the wiggler beamline BL17A at the National Synchrotron Radiation Research Center (NSRRC), Taiwan, by using a triangular bent Si(111) monochromator and a wavelength of 1.33320 Å. The sample in a 1 mm capillary was mounted on the Huber 5020 diffractometer. An air-stream heater was equipped at the BL17A beamline, and the temperature controller was programmed by a PC with a proportional-integral-derivative (PID) feedback system. Mass spectrometry data were obtained on a Finnigan MAT-95XL, and elemental analyses were performed on a Heraeus CHN-O-Rapid Analyzer at the NSC Regional Instrumental Center at the National Chiao Tung University, Hsinchu, Taiwan and at the National Cheng Kung University, Tainan, Taiwan.

*Hexakis(4-hexyloxyphenylethynyl)benzene (**1**):* To a mixture of *trans*-dichlorobis(triphenylphosphine)palladium(II) (38 mg, 0.05 mmol), copper iodide (21 mg, 0.11 mmol), triphenylphosphine (29 mg, 0.11 mmol), hexabromobenzene (300 mg, 0.54 mmol), and triethylamine (10 mL) was added 1-ethynyl-4-hexyloxybenzene (601 mg, 2.99 mmol) in triethylamine (15 mL) dropwise under a nitrogen atmosphere at reflux. The mixture was stirred at reflux for 7 h and then cooled. To the cooled reaction mixture was added dichloromethane (100 mL). The mixture was washed twice with aqueous NH_4Cl (200 mL), twice with H_2O (200 mL), and dried over $MgSO_4$. After removal of the solvents, the residue was purified by column chromatography (SiO_2, *n*-hexane/dichloromethane 7:1) and crystallized from *n*-hexane to yield **1** as a yellow powder

(104 mg, 0.081 mmol, yield 15 %). ^{1}H NMR (300 MHz,$CDCl_3$. δ): 7.55 (d, J = 8.7 Hz, 12H), 6.87 (d, J = 8.7 Hz, 12H), 3.99 (t, J = 6.3 Hz, 12H), 1.80 (m, 12H), 1.53–1.33 (m, 36H), 0.93 ppm (t, J = 6.9 Hz, 18H); ^{13}C NMR (75 MHz, $CDCl_3$, δ): 159.6, 133.3, 126.9, 115.4, 114.6, 99.1, 86.7, 68.1, 31.6, 29.2, 25.7, 22.6, 14.0 ppm; HRMS (FAB+, *m/z*): calcd for $C_{90}H_{102}O_6$, 1278.7676; found, 1278.7740. Anal. calcd for $C_{90}H_{102}O_6$: C 84.47, H 8.03; found: C 84.14, H 8.06.

*Hexakis(3-hexyloxyphenylethynyl)benzene (**2**):* By using the unique sidearm 1-ethynyl-2-hexyloxybenzene, **2** was obtained as a yellow powder in 46 % yield by a procedure similar to the procedure described for **1**. ^{1}H NMR (300 MHz, $CDCl_3$, δ): 7.25 (d, J = 5.4 Hz, 6H), 7.19 (s, 6H), 6.99–6.93 (m, 12H), 3.88 (t, J = 6.5 Hz, 12H), 1.75 (m, 12H), 1.51–1.33 (m, 36H), 0.93 ppm (t, J = 6.9 Hz, 18H); ^{13}C NMR (75 MHz, $CDCl_3$, δ): 160.4, 130.5, 128.5, 125.02, 125.00, 117.7, 117.6, 100.8, 87.7, 68.9, 32.8, 30.4, 26.9, 23.7, 14.6 ppm; HRMS (FAB+, *m/z*): calcd for $C_{90}H_{102}O_6$, 1278.7676; found, 1278.7705. Anal. calcd for $C_{90}H_{102}O_6$: C 84.47, H 8.03; found: C 84.46, H 8.04.

*Hexakis(2-hexyloxyphenylethynyl)benzene (**3**):* By using the unique sidearm 1-ethynyl-2-hexyloxybenzene, **3** was obtained as a yellow powder in 74 % yield by a procedure similar to the procedure described for **1**. ^{1}H NMR (300 MHz, $CDCl_3$, δ): 7.57 (dd, J = 7.5, 1.8 Hz, 6H), 7.25 (t, J = 7.8 Hz, 6H), 6.92 (d, J = 8.7 Hz, 6H), 6.83 (t, J = 7.5 Hz, 6H), 3.88 (t, J = 6.8 Hz, 12H), 1.47 (m, 12H), 1.30–1.08 (m, 36H), 0.81 ppm (t, J = 6.9 Hz, 18H); ^{13}C NMR (75 MHz, $CDCl_3$, δ): 159.9, 134.5, 129.6, 127.6, 119.9, 113.6, 112.4, 95.8, 91.4, 69.1, 31.4, 28.6, 25.4, 22.4, 13.9 ppm; HRMS (FAB+, *m/z*): calcd for $C_{90}H_{102}O_6$. 1278.7676; found, 1278.7699. Anal. calcd for $C_{90}H_{102}O_6$: C 84.47, H 8.03; found: C 84.48; H 8.06.

*1,3-Bis-(2-hexyloxyphenylethynyl)-2,4,5,6-tetrakis-(4-hexyloxyphenylethynyl)benzene (**4**):* To a mixture of *trans*-dichlorobis(triphenylphosphine)palladium(II) (5 mg, 0.007 mmol), copper iodide (3 mg, 0.016 mmol), triphenylphosphine (4 mg, 0.015 mmol), 1,3-dibromo-2,4,5,6-tetrakis(4-hexyloxyphenylethynyl)benzene (70 mg, 0.068 mmol), and triethylamine (10 mL) was added 1-ethynyl-2-hexyloxy-benzene (87 mg, 0.43 mmol) in triethylamine (10 mL) dropwise under a nitrogen atmosphere at reflux. The mixture was stirred at reflux for 14 h and then cooled. To the cooled reaction mixture was added dichloromethane (100 mL). The mixture was washed twice with aqueous NH_4Cl (200 mL), twice with H_2O (200 mL), and dried over $MgSO_4$. After removal of the solvents, the residue was purified by column chromatography (SiO_2, *n*-hexane/dichloromethane 4:1) and crystallized from *n*-hexane to yield **5** as a pale yellow powder (90 mg, 0.07 mmol, yield 67 %). ^{1}H NMR (300 MHz, $CDCl_3$, δ): 7.66–7.61 (m, 2H), 7.59–7.52 (m, 8H), 7.35–7.29 (m, 2H), 6.97–6.82 (m, 12H), 4.02–3.90 (m, 12H), 1.85–1.75 (m, 12H), 1.62–1.10 (m, 36H), 0.95–0.91 (m, 15H), 0.80 ppm (t, J = 7.1 Hz, 3H); ^{13}C NMR (75 MHz, $CDCl_3$, δ): 159.9, 159.6, 159.5, 134.3, 134.0, 133.5, 133.3, 130.0, 129.9, 127.3, 127.1, 127.0, 120.4, 120.2, 115.5, 115.4, 114.6, 114.5, 113.5, 113.4, 112.7, 112.6, 99.2, 99.0, 95.8, 95.6, 91.4, 91.3, 86.7, 69.3, 69.2, 68.1, 31.6, 31.5, 29.7, 29.2, 28.9, 28.8, 25.7, 25.4, 22.6, 22.5, 14.0 ppm. HRMS (FAB+, *m/z*): calcd for $C_{90}H_{102}O_6$, 1278.7676; found, 1278.7690.

*1-(2-Hexyloxyphenylethynyl)-2,3,4,5,6-pentakis(4-hexyloxyphenylethynyl)benzene (**5**):* To a mixture of *trans*-dichlorobis(triphenylphosphine)-palladium(II) (6 mg, 0.009 mmol), copper iodide (3 mg, 0.016 mmol), triphenylphosphine (4 mg, 0.015 mmol), 1-bromo-2,3,4,5,6-pentakis(4-hexyloxyphenylethynyl)benzene (122 mg, 0.105 mmol), and triethylamine (10 mL) was added 1-ethynyl-2-hexyloxybenzene (87 mg, 0.43 mmol) in triethylamine (10 mL) dropwise under a nitrogen atmosphere at reflux. The mixture was stirred at reflux for 14 h and then cooled. To the cooled reaction mixture was added dichloromethane (100 mL). The mixture was washed twice with aqueous NH_4Cl (200 mL, twice with H_2O (200 mL), and dried over $MgSO_4$. After removal of the solvents, the residue was purified by column chromatography (SiO_2, *n*-hexane/dichloromethane 4:1) and crystallized from *n*-hexane to yield **5** as a pale yellow powder (53 mg, 0.041 mmol, yield 61 %). ^{1}H NMR (300 MHz, $CDCl_3$, δ): 7.63 (dd, J = 3.8, 1.5 Hz, 1H), 7.56 (d, J = 11.7 Hz, 4H), 7.55 (d, J = 12.0 Hz, 2H), 7.53 (d, J = 12.0 Hz, 4H), 7.32 (m, 1H), 6.88 (m, 12H), 4.02-3.95 (m, 12H), 1.86–1.75 (m, 12H), 1.61–1.12 (m, 36H), 0.95–0.90 (m, 15H), 0.79 ppm (t, J = 6.8 Hz, 3H); ^{13}C NMR (75 MHz, $CDCl_3$, δ): 159.9, 159.62, 159.56, 134.0, 133.5, 133.3, 130.0, 127.2, 127.1, 127.0, 126.8, 120.4, 115.5, 115.4, 114.6, 114.5, 113.4, 112.7, 99.3, 99.1, 99.0, 95.6, 91.3, 86.7, 69.3, 68.14, 68.10, 31.6, 31.5, 29.2, 28.9, 25.7, 25.5, 22.6, 22.5, 14.0 ppm; HRMS (FAB+, *m/z*): calcd for $C_{90}H_{102}O_6$, 1278.7676; found, 1278.7698. Anal. calcd for $C_{90}H_{102}O_6$: C 84.47, H 8.03; found: C 84.38, H 8.03.

*1-(3-Hexyloxyphenylethynyl)-2,3,4,5,6-pentakis(4-hexyloxyphenylethynyl)benzene (**6**):* By using the unique sidearm 1-ethynyl-3-hexyloxybenzene, **6** was synthesized as a yellow powder in 56 % yield by a procedure similar to the procedure described for **5**. ^{1}H NMR (300 MHz, $CDCl_3$, δ): 7.50–7.60 (m, 10H), 7.15–7.30 (m, 2H), 7.11 (s, 1H), 6.80–7.00 (m, 11H), 3.90–4.10 (m, 10H), 3.85 (t, J = 6.8 Hz , 2H), 1.70–1.90 (m, 12H), 1.20–1.60 (m, 36H), 0.85–1.00 ppm (m, 18H); ^{13}C NMR (75 MHz, $CDCl_3$, δ): 160.3, 159.6, 133.8, 129.9, 127.7, 127.6, 127.3, 126.8, 124.6, 124.5, 117.0, 116.8, 115.4, 115.0, 99.9, 99.80, 99.76, 99.2, 87.9, 86.9, 86.84, 86.78, 68.6, 68.5, 32.11, 32.07, 29.74, 29.65, 26.2, 26.1, 23.1, 14.3 ppm; HRMS (FAB+, *m/z*): calcd for $C_{90}H_{102}O_6$, 1278.7676; found, 1278.7692. Anal. calcd for $C_{90}H_{102}O_6$: C 84.47, H 8.03; found: C 84.21, H 8.07.

*1-(3,4-Dihexyloxyphenylethynyl)-2,3,4,5,6-pentakis(4-hexyloxyphenylethynyl)benzene (**7**):* By using the unique sidearm 4-ethynyl-1,2-bis(hexyloxybenzene), **7** was obtained as a yellow powder in 42 % yield by a procedure similar to the procedure described for **5**. ^{1}H NMR (300 MHz, $CDCl_3$, δ): 7.50–7.60 (m, 10H), 7.19 (d, J = 8.4 Hz, 1H), 7.10 (s, 1H), 6.80–6.95 (m, 11H), 3.90–4.10 (m, 12H), 3.83 (t, J = 6.5 Hz, 2H), 1.70–1.90 (m, 14H), 1.20–1.60 (m, 42H), 0.92 ppm (t, J = 6.8 Hz, 21H); ^{13}C NMR (75 MHz, $CDCl_3$, δ): 159.6, 150.0, 148.9, 133.3, 127.0, 126.9, 125.1, 116.5, 115.6, 115.4, 114.6, 113.3, 99.4, 99.1, 99.0, 86.6, 86.4, 69.2, 69.0, 68.1, 31.6, 29.2, 25.7, 22.6, 14.0 ppm; HRMS (FAB+, *m/z*): calcd for $C_{96}H_{114}O_7$, 1378.8565; found, 1378.8586.

*1,2,3,4,5-Pentakis(4-hexyloxyphenylethynyl)-6-(2,3,4-trihexyloxyphenylethynyl)benzene (**8**):* By using the unique sidearm 1-ethynyl-2,3,4-trishexyloxybenzene, **8** was obtained as a yellow powder in 32 % yield by a procedure similar to the procedure described for **5**. ^{1}H NMR (300 MHz, $CDCl_3$, δ): 7.50–7.65 (m, 10H), 7.30 (d, J = 8.7 Hz, 1H), 6.80–6.95 (m, 10H), 6.62 (d, J = 8.7 Hz, 1H), 4.21 (t, J = 6.6 Hz, 2H), 3.90–4.10 (m, 14H), 1.70–2.00 (m, 16H), 1.00–1.70 (m, 48H), 0.85–1.00 (m, 21H), 0.78 ppm (t, J = 6.9 Hz, 3H); ^{13}C NMR (75 MHz, $CDCl_3$, δ): 159.6, 155.0, 154.6, 141.9, 133.5, 133.2, 128.5, 127.1, 126.9, 115.4, 114.6, 114.4, 110.7, 108.1, 99.2, 99.0, 95.9, 89.9, 86.7, 74.7, 73.8, 68.8, 68.1, 31.8, 31.6, 30.3, 30.2, 29.7, 29.3, 29.2, 25.8, 25.7, 22.6, 14.0 ppm; HRMS (FAB+, *m/z*): calcd for $C_{102}H_{126}O_8$, 1478.9453; found, 1479.9503. Anal. calcd for $C_{102}H_{126}O_8$: C 82.77, H 8.58; found: C 82.42, H 8.58.

*1,2,3,4,5-Pentakis(4-octylphenylethynyl)-6-(2,3,4-trihexyloxyphenylethynyl)benzene (**10**):* Cross-coupling 1-ethynyl-2,3,4-tris(hexyloxybenzene) to 1-bromo-2,3,4,5,6-pentakis(4-octylphenylethynyl)benzene using a procedure similar to the procedure described for **5** gave compound **8** as a yellow powder in 86 % yield. ^{1}H NMR (300 MHz, $CDCl_3$, δ): 7.60 (m, J = 7.8 Hz, 10H), 7.34 (d, J = 8.7 Hz, 1H), 7.10–7.25 (m, 10H), 6.64 (d, J = 8.7 Hz, 1H), 4.23 (t, J = 6.5 Hz, 2H), 4.00–4.10 (m, 4H), 2.60–2.75 (m, 10H), 0.75–2.00 ppm (m, 108H); ^{13}C NMR (75 MHz, $CDCl_3$, δ): 155.1, 154.6, 143.9, 143.8, 141.9, 132.0, 131.8, 128.5, 128.3, 127.5, 127.3, 127.3, 127.1, 120.6, 110.6, 108.1, 99.4, 99.3, 99.2, 96.3, 89.7, 87.2, 74.7, 73.87, 68.87, 36.07, 31.9, 31.8, 31.6, 31.2, 30.3, 30.2, 29.7, 29.5, 29.32, 29.26, 25.8, 25.8, 25.6, 22.7, 22.6, 14.1, 14.0 ppm; HRMS (FAB+, *m/z*): calcd for $C_{112}H_{146}O_3$, 1539.1272: found, 1539.1263. Anal. calcd for $C_{112}H_{146}O_3$: C 87.33, H 9.55; found: C 87.71, H 9.30.

Received: October 28, 2006
Revised: March 31, 2007
Published online: July 12, 2007

[1] a) H. Mori, Y. Itoh, Y. Nishiura, T. Nakamura, Y. Shinagawa, *Jpn. J. Appl. Phys.* **1997**, *36*, 143. b) K. Kawata, *Chem. Rec.* **2002**, *2*, 59.

[2] a) S. Kumar, K. Varshney, *Angew. Chem. Int. Ed.* **2000**, *39*, 3140. b) S. Chandrasekhar, S. Krishna Prasad, G. G. Nair, D. S. Shankar Rao, S. Kumar, M. Manickam, in *EuroDisplay '99, The 19th International Display Research Conference Late-News Papers*, Berlin **1999**, p. 9. c) S. Kumar, S. K. Varshney, D. Chauhan, *Mol. Cryst. Liq. Cryst.* **2003**, *396*, 241.

[3] a) A. N. Cammidge, R. J. Bushby, in *Handbook of Liquid Crystals, Vol. 2B* (Eds: D. Demus, J. Goodby, G. W. Gray, H.-W. Spiess, V. Vill), Wiley-VCH, Weinheim, Germany **1998**, Ch. 7. b) S. Chandrasekhar, in *Handbook of Liquid Crystals, Vol. 2B* (Eds: D. Demus, J. Goodby, G. W. Gray, H.-W. Spiess, V. Vill), Wiley-VCH, Weinheim, Germany **1998**, Ch. 8. c) K. Praefcke, B. Kohne, D. Singer, *Angew. Chem. Int. Ed. Engl.* **1990**, *29*, 177. d) M. Ebert, D. A. Jungbauer, R. Kleppinger, J. H. Wendorff, B. Kohne, K. Praefcke, *Liq. Cryst.* **1989**, *4*, 53. e) K. Praecfcke, D. Singer, B. Gundogan, K. Gutbier, M. Langner, *Ber. Bunsenges. Phys. Chem.* **1993**, *97*, 1358. f) S. Marguet, D. Markovitsi, D. Goldmann, D. Janietz, K. Praefcke, D. Singer, *J. Chem. Soc., Faraday Trans.* **1997**, *93*, 147. g) K. Praefcke, B. Kohne, K. Gutbier, N. Johnen, D. Singer, *Liq. Cryst.* **1989**, *5*, 233.

[4] M. W. Day, A. J. Matzger, R. H. Grubbs, personal communication.

[5] W. Weissflog, in *Handbook of Liquid Crystals, Vol. 2B* (Eds: D. Demus, J. Goodby, G. W. Gray, H.-W. Spiess, V. Vill), Wiley-VCH, Weinheim, Germany **1998**, Ch. 9.

[6] M. Lehmann, S.-W. Kang, C. Köhn, S. Haseloh, U. Kolb, D. Schollmeyer, Q.-B. Wang, S. Kumar, *J. Mater. Chem.* **2006**, *16*, 4326.

[7] a) V. De Cupere, J. Tant, P. Viville, R. Lazzaroni, W. Osikowicz, W. R. Salaneck, Y. H. Geerts, *Langmuir* **2006**, *22*, 7798. b) H. Meier, M. Lehmann, H. C. Holst, D. Schwöppe, *Tetrahedron* **2004**, *60*, 6881. c) P. Hindmarsh, M. J. Watson, M. Hird, J. W. Goodby, *J. Mater. Chem.* **1995**, *5*, 2111. d) C. D. Farve-Nicolin, J. Lub, P. van der Sluis, *Adv. Mater.* **1996**, *8*, 1005.

[8] B. Kohne, K. Praefcke, *Chimia* **1987**, *41*, 196.

[9] For example, hexakis(4-hexyloxy-phenylethynyl)benzene (**1**) showed an N_D phase between 144 and 216 °C; in contrast, hexakis(4-octylphenylethynyl)benzene (**9**) exhibited an N_D phase between 80 and 96 °C.

[10] The dimension of the hexakis(phenylethynyl)benzene core is calculated after geometry optimization by using the AM1 method and the molecular software PC Spartan Plus version 1.5.2 (Wavefunction, Inc.).

[11] M. Ebert, D. A. Jungbauer, R. Kleppinger, J. H. Wendorff, B. Kohne, K. Praefcke, *Liq. Cryst.* **1989**, *4*, 53.

[12] a) C. Suryanayana, M. G. Norton, in *X-ray Diffraction A Practical Approach*, Plenum Press, New York **1998**, p. 207. b) H. P. Klug, L. E. Alexander, in *X-ray Diffraction Procedures*, Wiley, New York **1981**. c) A. Grafe, D. Janietz, T. Frese, J. H. Wendorff, *Chem. Mater.* **2005**, *17*, 4979.

[13] P. H. J. Kouwer, W. F. Jager, W. J. Mijs, S. J. Picken, *Macromolecules* **2002**, *35*, 4322.

[14] M. Ebert, G. Frick, C. Baehr, J. H. Wendorff, R. Wüstefeld, H. Ringsdorf, *Liq. Cryst.* **1992**, *11*, 293.

[15] P. H. J. Kouwer, W. F. Jager, W. J. Mijs, S. J. Picken, *Macromolecules* **2000**, *33*, 4336.

[16] a) K. Praefcke, D. Singer, B. Kohne, M. Ebert, A. Liebmann, J. H. Wendorff, *Liq. Cryst.* **1991**, *10*, 147. b) D. Janietz, K. Praefcke, D. Singer, *Liq. Cryst.* **1993**, *13*, 247.

[17] M. Weck, A. R. Dunn, K. Matsumoto, G. W. Coates, E. B. Lobkovsky, R. H. Grubbs, *Angew. Chem. Int. Ed.* **1999**, *38*, 2741.

[18] K. Kobayashi, N. Kobayashi, *J. Org. Chem.* **2004**, *69*, 2487.